A QUANTITATIVE ANALYSIS OF TROPICAL CYCLONE FREQUENCY WITHIN THE ARABIAN SEA AND BAY OF BENGAL

by

Jessica M. Meyer, B.S.

A thesis submitted to the Graduate Council of
Texas State University in partial fulfillment
of the requirements for the degree of
Master of Science
with a Major in Geography
May 2022

Committee Members:

Richard Dixon, Chair

Ronald Hagelman

Denise Blanchard-Boehm

FAIR USE AND AUTHOR'S PERMISSION STATEMENT

Fair Use

Duplication Permission

ACKNOWLEDGEMENTS

I would like to express the deepest appreciation to my advisor, Dr. Richard Dixon, for the endless amount of time, patience, and guidance he has given me throughout the past two years. He continually displayed his passion for research and academia through his mentoring, and constantly challenged me to better myself academically. Without his support and persistence, this thesis would not have been possible.

I would also like to thank my committee members, Dr. Denise Blanchard-Boehm and Dr. Ron Hagelman, who demonstrated to me that broad thinking is just as beneficial in academia as it is in life. Dr. Blanchard-Boehm's expertise and kindness have been a major contributor to completing my degree and believing in myself. Learning from and working with Dr. Hagelman has been a crucial and an inspiring experience. I attribute much of my research interests and passion for environmental hazards to him.

I'd also like to thank Mrs. Allison Glass-Smith. Her emotional support, infinite emails, and wit have aided me through the highs and lows of this journey.

Lastly, thank you to my grandpa for being my biggest supporter and telling me to reach for the stars. You believed in me even when I did not believe in myself – I could not have done it without you.

TABLE OF CONTENTS

Page

ACKNOWLEDGEMENTS iv

LIST OF TABLES vii

LIST OF FIGURES viii

LIST OF ABBREVIATIONS ix

ABSTRACT x

CHAPTER

1. INTRODUCTION 1
   - 1.1 Research Problem 1
   - 1.2 Research Questions 3

2. LITERATURE REVIEW 4
   - 2.1 Tropical Cyclone Research 4
   - 2.2 Sea Surface Temperatures and the Indian Ocean Dipole 5
   - 2.3 Sea Surface Temperatures and the El Niño Southern Oscillation 7
   - 2.4 Consequences of Climate Change on Tropical Cyclones 8

3. DATA AND METHODS 11
   - 3.1 The North Indian Ocean Basin 11
     - 3.1.1 The Arabian Sea 12
     - 3.1.2 The Bay of Bengal 13
   - 3.2 Definitions 14
   - 3.3 Data 15
   - 3.4 Statistical Methods 21
     - 3.4.1 Descriptive Statistics 21
     - 3.4.2 Testing the Distribution of Data 21
     - 3.4.3 Trend Analysis 21
     - 3.4.4 Chi-Square Goodness of Fit Test 22
     - 3.4.5 Chi-Square Test of Independence 22

4. RESULTS 24

4.1 Descriptive Statistics: Establishing the Frequency of Tropical Cyclone Occurrences Over Time 24
4.2 Testing the Distribution of Data for Frequency of Occurrences Over Time 27
4.3 Trend Analysis for Temporal Frequency of Occurrences....................31
4.3.1 Regression Analysis of Cox-Stuart Trend 31
4.4 Chi-Square Goodness of Fit Test...36
4.5 Chi-Square Test of Independence..40

5. DISCUSSION 42

5.1 Descriptive Statistics: Temporal Changes in Frequency of Occurrences..42
5.2 Testing the Distribution of Data 42
5.3 Trend Analysis for Temporal Frequency of Occurrences....................43
5.3.1 Regression Analysis of Cox-Stuart Trend 43
5.4 Chi-Square Goodness of Fit Test...44
5.5 Chi-Square Test of Independence..45

6. CONCLUSION..46

REFERENCES 49

LIST OF TABLES

Table **Page**

3.3.1 Arabian Sea Tropical Cyclone Frequencies....17

3.3.2 Bay of Bengal Tropical Cyclone Frequencies....19

3.3.3 Transformed Indices Values....20

4.1.1 Descriptive Statistics for the Arabian Sea for entire period (1950 to 2020)....25

4.1.2 Descriptive Statistics for the Bay of Bengal for entire period (1950 to 2020)....26

4.3.1 Arabian Sea Cox-Stuart Analysis for Trend....32

4.3.2 Bay of Bengal Cox-Stuart Analysis for Trend....33

4.3.3 Regression Analysis....36

4.4.1 Chi-Square Goodness of Fit Test – ENSO and the Arabian Sea....38

4.4.2 Chi-Square Goodness of Fit Test – IOD and the Arabian Sea....38

4.4.3 Chi-Square Goodness of Fit Test – ENSO and the Bay of Bengal....39

4.4.4 Chi-Square Goodness of Fit Test – IOD and the Bay of Bengal....39

4.5 Chi-Square Test of Independence....41

LIST OF FIGURES

Figure **Page**

2.2 The Indian Ocean Dipole 7

2.3 The Southern Oscillation 9

3.1 The Northern Indian Ocean 11

3.1.1 The Arabian Sea...12

3.1.2 The Bay of Bengal 13

4.2.1 Arabian Sea Histogram 28

4.2.2 Bay of Bengal Histogram...28

4.2.3 Tropical Cyclone Events within the Arabian Sea 29

4.2.4 Tropical Cyclone Events within the Bay of Bengal..30

4.3.1 Regression Analysis of August Tropical Cyclones within the Bay of Bengal (1950 to 2020)..34

4.3.2 Regression Analysis of September Tropical Cyclones within the Bay of Bengal (1950 to 2020)..34

4.3.3 Regression Analysis of the Southwest Monsoon Season Tropical Cyclones within the Bay of Bengal (1950 to 2020)..35

4.3.4 Regression Analysis of Annual Tropical Cyclones within the Bay of Bengal (1950 to 2020)..35

LIST OF ABBREVIATIONS

Abbreviation	Description
IOD	Indian Ocean Dipole
ENSO	El Niño Southern Oscillation
H_0	Null Hypothesis
H_A	Alternate Hypothesis

ABSTRACT

This research examines characteristics, and trends, of tropical cyclone occurrences in the Northern Indian Ocean area between 1950 and 2020. Data from the India Meteorological Department was used to examine storm characteristics, while statistical analysis identified temporal trends. In addition, an attempt was made to identify the influence of the phase of the IOD and ENSO on tropical cyclone occurrences. Results from a Cox-Stuart non-parametric test found that there are significant trends in frequency of tropical cyclones within the Bay of Bengal during August, September, the Southwest Monsoon season (from June to September), and annually. Plotted regression analyses exhibited statistically significant slopes for September, the Southwest Monsoon season, and annually of -0.007, -0.016, and -0.028, respectively. No statistically significant trends were found within the Arabian Sea using the same alpha value of 0.025. The Chi-Square test of independence rejected the null hypothesis of IOD – ENSO independence during May, September, October, and the post-monsoon season with an alpha value of 0.001.

1. INTRODUCTION

1.1 Research Problem

Climate has influenced tropical cyclones. This has become more apparent in the most recent five decades during a time of exponential population growth, resource extraction and use (Knutson et al. 2020; IPCC AR6 2021). This study examined the historical records of tropical cyclone data in both the Arabian Sea and the Bay of Bengal, some of the most densely populated coastal areas in the world. The historical records of tropical cyclones may be utilized to find relevant patterns of potential prediction so that more resistant infrastructure, and accurate emergency management planning informed by the predictions, will help prevent future devastation and lives lost. The data utilized for this study is a partial historical record (1950-2020) downloaded from the India Meteorological Department online database that reports yearly counts of tropical cyclones for the Arabian Sea and Bay of Bengal. To analyze tropical cyclone frequencies, this study employed a Cox-Stuart trend analysis, a regression analysis of significant Cox-Stuart data, and a chi-square test of independence using JMP statistical software.

This research examined a dataset that had previously not been extensively analyzed to identify patterns of tropical storms in the Northern Indian Ocean. Information on such patterns may prove beneficial for these regional populations by informing and aiding mitigation management practices. The analysis of such a dataset will assist in plans for strengthening infrastructure to withstand more frequent tropical cyclone occurrence and thus, save lives, resources, and lessen long-lasting impacts. This research will also allow for the opportunity to advance scientific literature. Understanding the correlations and trends within this dataset will help predict future frequency expectancies for both areas of study and aid in preparedness for such storms.

In the recent Intergovernmental Panel on Climate Change Sixth Assessment Report (AR6 2021), the increasing greenhouse gas effect from anthropogenic sources is increasing sea surface temperatures and will continue to do so for upcoming centuries, suggesting a sharp increase in the strength of violent cyclonic activity within the next 50 years. While populations are exponentially growing, and demand for both physical space and resources creates development along coastlines around the world, the chances for disaster also increase. The statistical analyses used in this study were conducted with aspirations of discovering trends within the Arabian Sea and Bay of Bengal to aid at-risk populations within the surrounding areas, which may in turn be useful in improving standards for infrastructure to better mitigate tropical cyclone hazards.

The purpose of this study was to conduct a trend analysis of tropical cyclone frequency data and contribute new statistical information on the Bay of Bengal and Arabian Sea to the broader field of research. Few studies within these geographical areas of research have yet to exhibit a long-term trend of frequency without the use of general circulation modeling. The tropical cyclone data set of the Bay of Bengal and Arabian Sea from the India Meteorological Department was analyzed and examined for long-term trends which will promote mitigation for the future by establishing higher standards for infrastructure and emergency preparedness. While professionals within the field have discussed an increase in tropical cyclone intensity attributed to climate change, there is a need for more frequency analyses within the Bay of Bengal and Arabian Sea because this may impact recovery time from previous tropical cyclones if proper and insufficient mitigation are practiced along these coastal areas.

1.2 Research Questions

This study aimed to answer the following questions for each study area:

1) Are there temporal trends in tropical cyclone frequency from 1950 to 2020?
2) If so, are the trends increasing or decreasing? During which months or seasons does this occur?
3) Is there a statistically significant relationship between the Indian Ocean dipole, the Southern Oscillation, and tropical cyclone frequency?

2. LITERATURE REVIEW

2.1 Tropical Cyclone Research

Most of all tropical cyclone damage in the past century resulted from rapid intensification, “an increase in maximum sustained winds of a tropical cyclone of at least 30 knots in a 24-hour period,” prior to landfall (Glossary of NHC Terms n.d.; Bhatia et al. 2018). Global tropical cyclone frequency has increased since the early 1900s due to such factors as the warming of both the atmosphere and oceans, increased tropical depression formation, and improvements in detection (Fitchett 2018). Climate change also impacts frequency and distribution of tropical cyclones around the world, dependent upon atmospheric circulation, ocean thermodynamics, and geologic environmental influences (Henderson-Sellers et al. 1998). Additionally, due to global warming, the centers or eyes of tropical cyclones are increasing vertically in both temperature and humidity leading to an increase in intensity due to greater available potential energy (Mittal et al. 2019). Rainfall averages and extremes from tropical cyclones have also increased due to the increase of potential energy from heating and cover a more extensive spatial area (Collins and Walsh 2017). Climate change exhibits a domino effect on tropical cyclone genesis and promotion around the world and continues to do so as atmospheric and oceanic temperatures continuously rise.

The National Hurricane Center began issuing wind speed forecasts of tropical cyclones in 2006 based on extrapolations from previous storms, and but has yet to develop a model for predicting tropical storm intensity and structure due to lack of satellite imagery resolution (Lee et al. 2015). Several models have been utilized to try and predict the intensity and frequencies of tropical cyclones in various parts of the world.

The most commonly used are the atmospheric general circulation model and the general circulation model which are based upon environmental variables, both long- and short-term. These models, however, do not account for variables such as wind-induced ocean mixing or post-tropical cyclone cooled ocean waters, and are based upon replicated controlled experiments under parameters that may not be germane to all tropical cyclones within the study (Bhatia et al. 2018). Multiple linear regression analyses are performed in several studies to set up the models and use a subset of data in each study instead of the full dataset for the study area, limiting the results and possibly skewing results away from true outliers (Lee et al. 2015). Each study determined that intensity and frequency are increasing and will continue to do so based upon the experimental models and the observed environmental variables. However, few studies within the field have yet to exhibit a long-term trend of frequency outside of a circulation model, and furthermore, any statistical analyses allow room for error due to temporal inconsistencies within the available datasets (Kossin, Olander, and Knapp 2013).

2.2 Sea Surface Temperatures and the Indian Ocean Dipole

While climate change may not directly influence the frequency or intensity of tropical cyclones, it does cause shifts in atmospheric temperatures and sea surface temperatures, which all directly influence the genesis of all storm formations. Additionally, warming of ocean temperatures is the result of warmer sea surface temperatures being mixed downwards via vertical turbulence (Wells 2012). According to Du and Xie (2008), sea surface temperature within the upper 125 meters of the tropical Indian Ocean have been increasing in the recent 70 years, with an average sea surface temperature increase by half a degree Celsius. Shifts in the tropical Indian Ocean sea surface temperature are influenced by ENSO but can influence other global oscillations as well (Zhang et al. 2021). Furthermore, Yang et al. (2007) explored the plausible relationship between tropical Indian Ocean sea surface temperature increases and global climate. The fluctuation of sea surface temperature within the Indian Ocean Basin leads to many uncertainties when predicting tropical cyclone patterns. Each oceanic basin and its oscillations create additional variation when attempting to analyze patterns and chart overall changes in global frequency or intensity of tropical cyclones (Murakami, Mizuta and Shindo 2012).

The Indian Ocean sea surface temperature variability is impacted by the Indian Ocean dipole (Figure 2.2.1). It is exhibited interannually and creates a fluctuation of warming and cooling throughout the tropical Indian Ocean, with the fluxes generally occurring three to six months following the El Niño Southern Oscillation cycle, due to cloud, surface, precipitation, and evaporation variations (Klein, Soden and Lau 1999). The Indian Ocean dipole is a shift of sea surface temperatures from East to West (Saji et al. 1999), with some previous models claiming that the dipole shift is caused by ENSO and others claim is independent, leaving an uncertainty census within the field (Zhang et al. 2021). Additionally, the Indian Ocean dipole has complementary wind and precipitation anomalies, leading to the discovery of a specifically strong atmospheric-oceanic interaction (Saji et al. 1999). Zheng et al. (2013) states that the Indian Ocean dipole sea surface variance is dependent upon depth shifts in the thermocline and oceanic-atmospheric feedback within the Basin. Consequently, Yuan and Cao (2013) relate the Indian Ocean dipole to tropical cyclones of the North Indian Ocean due to shifts in sea surface temperatures. Tropical cyclones are dependent upon warm sea

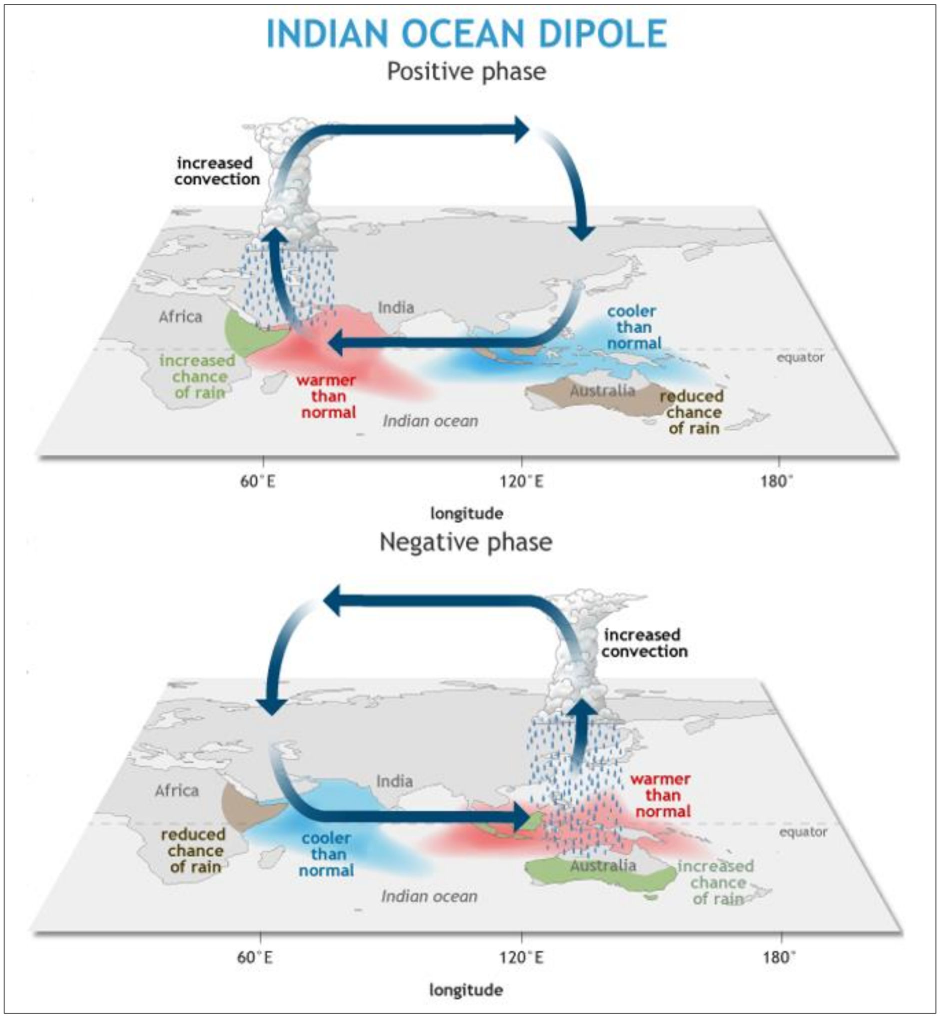

Figure 2.2 The Indian Ocean Dipole. The coupling of the atmosphere and ocean processes shown for both the positive (cool) phase and negative (warm) phase of the Indian Ocean Dipole phenomenon with increased convection over warmer waters and a decrease of precipitation over cooler waters (Johnson 2020).

surface temperatures for genesis and subsequent energy necessary to manifest into a destructive strength.

2.3 Sea Surface Temperatures and the El Niño Southern Oscillation

The first known official recognition of the Southern Oscillation was recorded in 1924 by Gilbert Walker, and further research by Jacob Bjerknes explained some of the climatic patterns and mechanisms of such Southern Oscillation events (Bjerknes 1966;

Cushman 2003). Bjerknes (1966) describes the atmospheric-oceanic coupling phenomenon and referenced warm or cold ocean undercurrents in relation to the atmospheric Hadley cells. He also goes on to examine an extremely weak easterly wind event that resulted in the elimination of oceanic upwelling and noted equatorial sea surface temperature anomalies that occur in the eastern Pacific Ocean that play an influential role in both seasonal and climatic anomalies. El Niño or ENSO is characterized as an atmospheric-oceanic coupling mechanism that causes warmer than average sea surface temperatures along the equatorial Pacific Ocean, specifically along the north-western coast of South America and the east coast of the African continent, with more convection occurring in Europe and along the west coast of North America (Figure 2.3.1). During El Niño, trade winds weaken which allow warmer than average water to move into the eastern and central Pacific Ocean (L'Heureux 2014). El Niño is considered the warm or negative phase of the Southern Oscillation, occurring less frequently than its' opposite phase, La Niña. While the term El Niño was coined in the early 1900's, the cooler than average sea surface temperature or positive phase of the Southern Oscillation, La Niña, was not described until the 1980's (Halpert et al. 2016). Lastly, the neutral phase of the Southern Oscillation has average Pacific Walker cell circulation patterns with average sea surface temperatures occurring. However, sea surface temperature anomalies can still occur, but without oceanic-atmospheric coupling, the Southern Oscillation will remain in a neutral phase.

2.4 Consequences of Climate Change on Tropical Cyclones

Beginning with, and continuing through the pre-industrial era, anthropogenic greenhouse gas emissions have exponentially increased concentrations of carbon dioxide

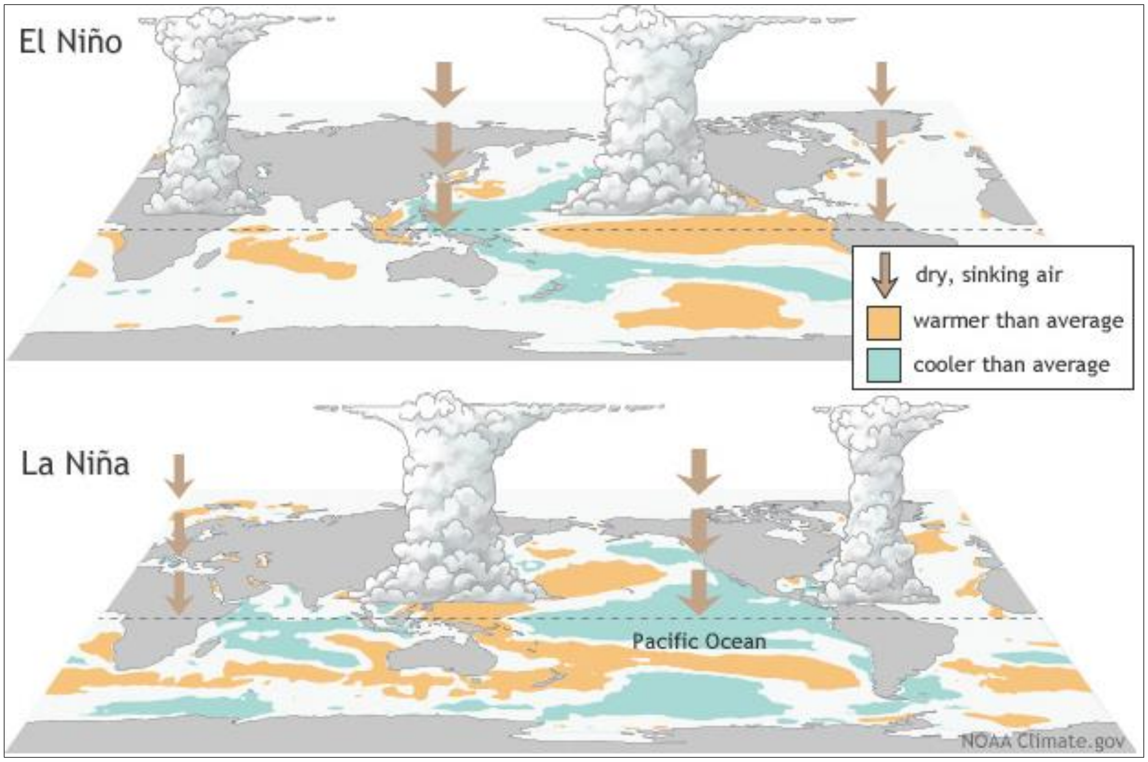

Figure 2.3 The Southern Oscillation. The coupling of the atmosphere and ocean processes shown for both the positive (La Niña) phase and negative (El Niño) phase of the Southern Oscillation with increased convection over warmer waters and a decrease of precipitation over cooler waters (El Nino and La Nina 2021).

(CO_2), methane (CH_4), and nitrous oxide (N_2O). While the greenhouse gas emission sinks such as the forests and oceans have consistently taken up about 56 percent of emissions, temperatures within the previous four decades have successively warmed approximately 0.68°C to 1.01°C (regionally dependent) (Intergovernmental Panel on Climate Change Sixth Assessment Report 2021).

According to the IPCC Fifth Assessment Report (2013), "The ocean has absorbed about 93% of the combined heat stored by warmed air, sea, and land, and melted ice between 1971 and 2010." This directly leads to warming of the oceans and increased the amounts of available energy for tropical cyclone evolution. While Category one, two, and three hurricanes (on the Saffir-Simpson scale) have decreased between 1970 and 2005, the percentage of Category four and five hurricanes has increased from 16 percent to 35 percent globally, and from eight percent to 25 percent within the Northern Indian Ocean (Webster et al. 2005). Analyzing previous trends is crucial to understanding what influences tropical cyclone events, and how those influences have shifted over time. Greenhouse gas emissions will continue to rise due to anthropogenic activity causing the warming to increase, with the majority of the heat energy being absorbed by oceans. This cyclical effect will continue for the upcoming centuries, providing more potential energy within the oceans, consequentially yielding more frequent and more violent tropical cyclones.

3. DATA AND METHODS

3.1 The North Indian Ocean Basin

For this research, the area of study is the Northern Indian Ocean, an oceanic basin that encompasses the Arabian Sea and the Bay of Bengal and produces tropical cyclones throughout the year (Ankur et al. 2020; Figure 3.1). The Indian Ocean has an important regional and global climate influence due to the process of basin warming known as the Indian Ocean Dipole mode. Paul and Rashid (2017) define the Indian Ocean Dipole mode as an ocean-atmospheric circulation anomaly when warm and cool pools of water shift between east and west, influencing rainfall, storms, and wind patterns. Basin warming is exaggerated when coupled with the El Niño-Southern Oscillation. The Indian Ocean Dipole mode sea surface temperature anomaly greatly influences circulation in the ocean and atmosphere, prompting global climate anomalies (Saji et al. 1999; Clark, Webster, and Cole 2003; Saji and Yamagata 2003). The areas of study for the purposes of this research are the Arabian Sea and the Bay of Bengal.

Figure 3.1 The Northern Indian Ocean (Esri).

3.1.1 The Arabian Sea

The Arabian Sea is located between the Arabian Peninsula and the Indian Subcontinent, with a maximum width of 2400 kilometers and depth of 5030 meters (Arabian Sea 2018; Figure 3.1.1). Tropical cyclones within the Arabian Sea are typically less intense and more infrequent when compared to the Bay of Bengal, but influence regional climates when they do occur, generally during May, June, November, and December (Rafiq, Blaschke, and Tajbar 2015). The basin is influenced by unilateral wind systems created during monsoon seasons that shift during semiannual tropical cyclone seasons (Chowdhury et al. 2020).

Figure 3.1.1 The Arabian Sea (Esri).

3.1.2 The Bay of Bengal

The Bay of Bengal is located between the Indian Subcontinent and Malay Peninsula, with a maximum width of 1610 kilometers, maximum length of 2090 kilometers, and maximum depth of 4694 meters (Bay of Bengal n.d.; Bay of Bengal 2018; Figure 3.1.2). Ali (1979) attributed devastating storm surge from tropical cyclones to low bathymetry, bay convergence, regularly high ocean tides, dense coastal populations, tropical cyclone paths, and large river systems. The Bay of Bengal continuously observes the highest storm surges on Earth with a decadal average of more than five meters (Needham, Keim, and Sathiaraj 2015).

Figure 3.1.2 The Bay of Bengal (Esri).

3.2 Definitions

Some definitions are required for comprehension of the upcoming data and methods:

- Tropical Cyclone – a tropical storm forming between 5º and 25º North or South of the equator consisting of a low-pressure center and rotating winds greater than 34 knots sustained for three minutes (Hyndman and Hyndman 2017; India Meteorological Department 2020)
- Indian Ocean Dipole (IOD) – a tropical teleconnection with a seesaw effect occurring within the Indian Ocean consisting of three phases (Johnson 2020)
    - Positive phase – sea surface temperatures are abnormally warm in the western Indian Ocean and abnormally cool in the eastern Indian Ocean
    - Negative phase – sea surface temperatures are abnormally warm in the eastern Indian Ocean and abnormally cool in the western Indian Ocean
    - Neutral phase – no sea surface temperature anomalies
- El Niño Southern Oscillation (ENSO) – A tropical teleconnection with a seesaw effect of atmospheric and oceanic coupling occurring within the equatorial Pacific Ocean consisting of three phases (El Nino and La Nina 2021)
    - Positive phase (La Niña) – sea surface temperatures are abnormally warm in the western equatorial Pacific Ocean and abnormally cool in the eastern equatorial Pacific Ocean

  - Negative phase (El Niño) – sea surface temperatures are abnormally warm in the eastern equatorial Pacific Ocean and abnormally cool in the western equatorial Pacific Ocean
  - Neutral phase – no sea surface temperature anomalies or no atmospheric-oceanic coupling when anomalies occur
- Seasons as defined by the India Meteorological Department (2020):
  - Winter – January and February
  - Pre-Monsoon – March, April, and May
  - Southwest Monsoon – June, July, August, and September
  - Post-Monsoon – October, November, and December

3.3 Data

This research utilizes data retrieved from the India Meteorological Department's online public database in March of 2021 (Table 3.3.1 and Table 3.3.2). The India Meteorological Department was established in 1875 with the goal of uniting all meteorological work within the country under one authority in New Delhi. Historical tropical cyclone records for the North Indian Ocean began in 1891 and include totals for each month and each year, through 2020, as well as the totals for the two study areas – the Arabian Sea and the Bay of Bengal – per month per year. However, only data from 1950 through 2020 is utilized. It should be noted that early data may be skewed due to lack of technological ability to detect tropical cyclones. The first tropical storm documented via satellite was not until 1961, so prior tropical cyclone data was based on surface measurements and ship observations (NOAA 2019; McAdie et al. 2009).

In addition, IOD and ENSO index was retrieved from the National Oceanic and Atmospheric Administration free online database in April of 2021 in the form of indices spanning 1866 through 2020. Again, only 1950 through 2020 data was utilized. To create uniform datasets, the data within each index was transformed into integers based on sea surface temperature anomaly (Table 3.3.3). The interaction of the IOD phase and ENSO phase transformative data was utilized during the chi-square statistical analysis.

Table 3.3.1 Arabian Sea Tropical Cyclone Frequencies. Tropical cyclone frequency per month beginning in 1950 through 2020 (India Meteorological Department 2020).

Arabian Sea												
Year	*J*	*F*	*M*	*A*	*M*	*J*	*J*	*A*	*S*	*O*	*N*	*D*
1950	0	0	0	0	0	0	0	0	0	0	0	0
1951	0	0	0	1	0	0	0	0	0	0	1	0
1952	0	0	0	0	0	0	0	0	0	0	0	0
1953	0	0	0	0	0	0	0	0	0	0	0	0
1954	0	0	0	0	0	0	0	0	0	0	0	0
1955	0	0	0	0	0	0	0	0	0	0	0	0
1956	0	0	0	0	0	0	0	0	0	0	0	0
1957	0	0	0	0	0	0	0	0	0	0	1	0
1958	0	0	0	0	0	0	0	0	0	0	0	0
1959	0	0	0	0	1	1	0	0	0	1	0	0
1960	0	0	0	0	1	0	0	0	0	0	1	0
1961	0	0	0	0	1	1	0	0	0	0	0	0
1962	0	0	0	0	0	0	0	0	0	0	0	0
1963	0	0	0	0	1	0	0	0	0	1	0	1
1964	0	0	0	0	0	1	0	1	0	0	1	0
1965	0	0	0	0	0	0	0	0	0	0	0	1
1966	0	0	0	0	0	0	0	0	1	0	0	0
1967	0	0	0	0	0	0	0	0	0	0	0	0
1968	0	0	0	0	0	0	0	0	0	0	0	0
1969	0	0	0	0	0	0	0	0	0	0	0	0
1970	0	0	0	0	1	0	0	0	0	0	1	0
1971	0	0	0	0	0	0	0	0	0	1	0	1
1972	0	0	0	0	0	0	0	0	0	1	0	0
1973	0	0	0	0	0	1	0	0	0	0	0	0
1974	0	0	0	1	1	0	0	0	1	0	0	0
1975	0	0	0	0	1	0	0	0	0	1	0	0
1976	0	0	0	0	1	0	0	0	0	1	0	0
1977	0	0	0	0	0	1	0	0	0	0	0	0
1978	0	0	0	0	0	0	0	0	0	0	0	0
1979	0	0	0	0	0	1	0	0	1	0	0	0
1980	0	0	0	0	0	0	0	0	0	0	0	0
1981	0	0	0	0	0	0	0	0	0	1	0	0
1982	0	0	0	0	0	0	0	0	0	0	1	0
1983	0	0	0	0	0	0	0	0	0	0	0	0
1984	0	0	0	0	0	0	0	0	0	0	0	0
1985	0	0	0	0	1	0	0	0	0	0	0	0
1986	0	0	0	0	0	0	0	0	0	0	0	0
1987	0	0	0	0	0	0	0	0	0	0	0	0
1988	0	0	0	0	0	0	0	0	0	0	0	0
1989	0	0	0	0	0	0	0	0	0	0	0	0
1990	0	0	0	0	0	0	0	0	0	0	0	0

Arabian Sea Continued												
Year	*J*	*F*	*M*	*A*	*M*	*J*	*J*	*A*	*S*	*O*	*N*	*D*
1991	0	0	0	0	0	0	0	0	0	0	0	0
1992	0	0	0	0	0	1	0	0	0	1	0	0
1993	0	0	0	0	0	0	0	0	0	0	1	0
1994	0	0	0	0	0	1	0	0	0	0	1	0
1995	0	0	0	0	0	0	0	0	0	1	0	0
1996	0	0	0	0	0	1	0	0	0	1	0	0
1997	0	0	0	0	0	0	0	0	0	0	0	0
1998	0	0	0	0	0	1	0	0	0	1	0	1
1999	0	0	0	0	1	0	0	0	0	0	0	0
2000	0	0	0	0	0	0	0	0	0	0	0	0
2001	0	0	0	0	1	0	0	0	1	1	0	0
2002	0	0	0	0	1	0	0	0	0	0	0	0
2003	0	0	0	0	0	0	0	0	0	0	1	0
2004	0	0	0	0	1	0	0	0	1	0	1	0
2005	0	0	0	0	0	0	0	0	0	0	0	0
2006	0	0	0	0	0	0	0	0	1	0	0	0
2007	0	0	0	0	0	2	0	0	0	0	0	0
2008	0	0	0	0	0	0	0	0	0	0	0	0
2009	0	0	0	0	0	0	0	0	0	0	1	0
2010	0	0	0	0	2	0	0	0	0	0	0	0
2011	0	0	0	0	0	0	0	0	0	1	0	1
2012	0	0	0	0	0	0	0	0	0	1	0	0
2013	0	0	0	0	0	0	0	0	0	0	0	0
2014	0	0	0	0	1	0	0	0	0	1	0	0
2015	0	0	0	0	0	1	0	0	0	1	1	0
2016	0	0	0	0	0	0	0	0	0	0	0	0
2017	0	0	0	0	0	0	0	0	0	0	0	0
2018	0	0	0	0	2	0	0	0	0	1	0	0
2019	0	0	0	0	0	1	0	0	1	2	0	1
2020	0	0	0	0	0	1	0	0	0	0	1	0

By using transformed values from the IOD and ENSO indices, the chi-square analysis examined the relationship between the warm, cool, and neutral phases of both the Indian and Pacific ocean basins during time periods of frequent and infrequent tropical cyclones.

Table 3.3.2 Bay of Bengal Tropical Cyclone Frequencies. Tropical cyclone frequency per month beginning in 1950 through 2020 (India Meteorological Department 2020).

Bay of Bengal												
Year	*J*	*F*	*M*	*A*	*M*	*J*	*J*	*A*	*S*	*O*	*N*	*D*
1950	0	0	0	0	0	1	0	0	1	0	1	1
1951	0	0	0	0	0	0	1	0	0	0	0	1
1952	0	0	0	0	1	0	1	0	0	0	2	0
1953	0	0	0	1	0	0	0	0	0	0	0	0
1954	0	0	0	0	0	0	0	0	1	0	0	0
1955	0	0	0	0	1	0	0	0	2	1	2	0
1956	0	0	0	1	1	1	0	0	0	1	0	0
1957	0	0	0	0	0	0	0	1	0	0	0	1
1958	0	0	0	0	1	0	0	0	0	2	2	0
1959	0	0	0	0	0	1	1	0	1	0	0	0
1960	0	0	0	0	1	0	0	0	0	2	0	0
1961	0	0	0	0	2	0	0	0	1	0	0	0
1962	0	0	0	0	1	0	0	0	0	1	1	1
1963	0	0	0	0	1	0	0	0	0	2	0	0
1964	0	0	0	0	1	0	0	0	0	0	2	1
1965	0	0	0	0	2	0	0	0	0	0	1	2
1966	0	0	0	1	0	0	0	0	1	0	4	1
1967	1	0	0	0	1	0	0	0	0	3	0	1
1968	0	0	0	0	1	0	0	0	2	1	2	1
1969	0	0	0	0	1	0	0	1	0	2	1	1
1970	0	0	0	0	1	1	0	0	0	1	1	0
1971	0	0	0	0	1	1	0	0	1	1	1	0
1972	0	0	0	1	0	0	1	0	1	0	1	1
1973	0	0	0	0	0	0	1	0	0	1	2	1
1974	0	0	0	0	1	0	0	1	1	0	1	0
1975	0	0	0	0	1	1	0	0	0	0	3	0
1976	0	0	0	1	0	0	0	0	1	1	3	1
1977	0	0	0	0	1	0	0	0	0	1	2	0
1978	0	0	0	0	1	0	0	1	0	1	2	0
1979	0	0	0	0	1	0	0	1	0	0	1	0
1980	0	0	0	0	0	0	0	0	0	1	0	2
1981	0	0	0	0	0	0	0	1	1	0	2	1
1982	0	0	0	0	2	0	0	0	0	2	0	0
1983	0	0	0	0	0	0	0	0	0	2	1	0
1984	0	0	0	0	0	0	0	0	0	1	2	0
1985	0	0	0	0	1	0	0	0	1	2	1	1
1986	0	0	0	0	0	0	0	0	0	0	1	0
1987	1	0	0	0	0	1	0	0	0	2	1	0
1988	0	0	0	0	0	0	0	0	0	1	2	0
1989	0	0	0	0	1	0	1	0	0	0	1	0
1990	0	0	0	0	1	0	0	0	0	0	0	1

Bay of Bengal Continued												
Year	*J*	*F*	*M*	*A*	*M*	*J*	*J*	*A*	*S*	*O*	*N*	*D*
1991	0	0	0	1	1	0	0	0	0	0	1	0
1992	0	0	0	0	1	0	0	0	0	0	3	0
1993	0	0	0	0	0	0	0	0	0	0	0	1
1994	0	0	0	1	0	0	0	0	0	1	0	0
1995	0	0	0	0	0	0	0	0	0	0	2	0
1996	0	0	0	0	0	1	0	0	0	0	2	0
1997	0	0	0	0	1	0	0	0	1	0	1	0
1998	0	0	0	0	1	0	0	0	0	0	2	0
1999	0	1	0	0	0	0	0	0	0	2	0	0
2000	0	0	1	0	0	0	0	0	0	1	1	1
2001	0	0	0	0	0	0	0	0	0	1	0	0
2002	0	0	0	0	0	0	0	0	0	0	2	1
2003	0	0	0	0	1	0	0	0	0	0	0	1
2004	0	0	0	0	1	0	0	0	0	0	0	0
2005	1	0	0	0	0	0	0	0	1	0	1	1
2006	0	0	0	1	0	0	0	0	0	1	0	0
2007	0	0	0	0	1	0	0	0	0	0	1	0
2008	0	0	0	1	0	0	0	0	0	1	1	0
2009	0	0	0	1	1	0	0	0	0	0	0	1
2010	0	0	0	0	1	0	0	0	0	1	1	0
2011	0	0	0	0	0	0	0	0	0	0	0	0
2012	0	0	0	0	0	0	0	0	0	1	0	0
2013	0	0	0	0	1	0	0	0	0	1	2	1
2014	0	0	0	0	0	0	0	0	0	1	0	0
2015	0	0	0	0	0	0	1	0	0	0	0	0
2016	0	0	0	0	1	0	0	0	0	1	1	1
2017	0	0	0	1	1	0	0	0	0	0	1	0
2018	0	0	0	0	0	0	0	0	1	1	1	1
2019	1	0	0	1	0	0	0	0	0	0	1	0
2020	0	0	0	0	1	0	0	0	0	0	1	1

Table 3.3.3 Transformed Indices Values. The transformative indices values used to create numerically uniform IOD and ENSO integers utilized during the chi-square analysis (National Oceanic and Atmospheric Administration 2022).

Phase	*Integers*	*IOD Index*	*ENSO Index*
Warm	-1	≤ -0.35	≤ 0.75
Neutral	0	-0.34 – 0.34	-0.74 – 0.74
Cool	1	≥ 0.35	≤ -0.75

3.4 Statistical Methods

3.4.1 Descriptive Statistics

The descriptive statistics (mean, median, variance, maximum, minimum, and standard deviation) were calculated for both the study areas using monthly, seasonal, and annual tropical cyclone occurrences. All descriptive statistics were calculated using the 1950 through 2020 tropical cyclone occurrences.

3.4.2 Testing the Distribution of Data

To determine which comparative test was the best to use for this dataset, 1950 to 2020, the tropical cyclone frequencies were plotted to exhibit the shape of the distribution for each study area. Shape was used to determine if the dataset is considered normal or non-normal. The data utilized within this study was found to not follow the normal curve or distribution for either study area and, therefore, non-parametric tests were required for this analysis.

3.4.3 Trend Analysis

A Cox-Stuart non-parametric test was used to determine any statistically significant temporal trends using tropical cyclone occurrences from 1950 to 2020, with the year of 1985 omitted due to the odd number of years. The entire sample period was utilized for each study area and for each variable (month, season, annual). The Cox-Stuart test for temporal trend requires early observations paired with later observations, and therefore omitting the middle observation yields equal observations for pairs (Daniel 1978). The positive or negative difference was calculated between each observation pair, omitting the pairs that exhibited no difference. Lastly, the lesser number of positive or negative signs coupled with the total number of signs were used with the binomial probability distribution table to yield a p-value.

A regression slope was plotted and calculated using the software statistical program JMP for each statistically significant p-value that was less than the alpha value of 0.025 during the Cox-Stuart temporal trend test. Additionally, the p-value for each regression slope was calculated to determine regression slope significance.

3.4.4 Chi-Square Goodness of Fit Test

A Chi-Square Goodness of Fit test was used for the entire sample period of 1950 to 2020, using tropical cyclone frequency data and both transformed indices containing IOD and ENSO anomalies. This test statistic compares expected and observed frequencies to determine if the observed frequencies follow the expected distribution of frequencies (Daniel 1978) and for the purposes of this research, to determine impact of IOD and ENSO phase on tropical cyclone occurrences. The percentage of years per ENSO and IOD phase was calculated for all variables (month, season, annual) and multiplied by the tropical cyclone frequency to attain the expected values for use in the chi-square equation. Examining the critical value of $\alpha = 0.025$ is 7.378, using two degrees of freedom. The null hypothesis (H_0) indicates that the observed tropical cyclone frequencies follow the expected distribution. The alternate hypothesis (H_A) indicates that the observed tropical cyclone frequencies do not follow the expected distribution.

3.4.5 Chi-Square Test of Independence

The last analysis was a Chi-Square Test of Independence using the transformed IOD ENSO indices and tropical cyclone occurrences. This test assesses whether two variables are associated or related with one another, or if the variables are independent of one another (Daniel 1978). This analysis examined nine phase possibilities (IOD -1, 0, 1 * ENSO -1, 0, 1) for all variables (months, seasons, and annual), comparing the observed and expected tropical cyclone frequencies. Two degrees of freedom with $\alpha = 0.005$ yielded a critical value of 14.86.

4. RESULTS

4.1 Descriptive Statistics: Establishing the Frequency of Tropical Cyclone Occurrences Over Time

The sample of data from 1950 to 2020 provided 71 years of tropical cyclone occurrence data. The statistical variables indicated several apparent differences between the Arabian Sea and the Bay of Bengal. One such difference was the total number of tropical cyclones that occurred during the entire sample period (71 years) within the Arabian Sea (81; Table 4.1) and the Bay of Bengal (242; Table 4.2). It should be noted that the Arabian Sea had a lower range during all variables except April, May, June, August, and the pre-monsoon season, with only the June variable exhibiting a greater range of tropical cyclone occurrences than the Bay of Bengal (Table 4.1 and 4.2). The Arabian Sea pre-monsoon season reported no occurrences throughout the entire period while the Bay of Bengal pre-monsoon season had six occurrences, exhibiting a more active area during the lowest yielding season.

The minimum number of tropical cyclones for both study areas was zero for all variables and the maximum number of tropical cyclones was consistently higher in the Bay of Bengal for all months and seasons. All monthly and seasonal means were higher in the Bay of Bengal, except for June, which had a mean of 0.113 compared to a mean of 0.211 and almost doubled the number of occurrences in the Arabian Sea (Table 4.1 and Table 4.2). Variance and standard deviation were both higher in Bay of Bengal for all months and seasons.

Table 4.1.1 Descriptive Statistics for the Arabian Sea for entire period (1950 to 2020).

Arabian Sea																	
Descriptive Statistics	*J*	*F*	*M*	*A*	*M*	*J*	*J*	*A*	*S*	*O*	*N*	*D*	*JF*	*MAM*	*JJAS*	*OND*	*Ann*
Number of Observations	71	71	71	71	71	71	71	71	71	71	71	71	71	71	71	71	71
Tropical Cyclone Occurrences	0	0	0	2	18	15	0	1	7	19	13	6	0	20	23	38	81
Mean	0	0	0	.028	.254	.211	0	.014	.099	.268	.183	.085	0	.282	.324	.535	1.141
Median	0	0	0	0	0	0	0	0	0	0	0	0	0	0	0	0	1
Minimum	0	0	0	0	0	0	0	0	0	0	0	0	0	0	0	0	0
Maximum	0	0	0	1	2	2	0	1	1	2	1	1	0	2	2	3	5
Variance	0	0	0	.028	.249	.198	0	.014	.090	.227	.152	.078	0	.290	.336	.481	1.351
Standard Deviation	0	0	0	.167	.499	.445	0	.119	.300	.477	.390	.280	0	.539	.580	.693	1.162

Table 4.1.2 Descriptive Statistics for the Bay of Bengal for entire period (1950 to 2020).

Bay of Bengal																	
Descriptive Statistics	*J*	*F*	*M*	*A*	*M*	*J*	*J*	*A*	*S*	*O*	*N*	*D*	*JF*	*MAM*	*JJAS*	*OND*	*Ann*
Number of Observations	71	71	71	71	71	71	71	71	71	71	71	71	71	71	71	71	71
Tropical Cyclone Occurrences	4	1	1	12	40	8	7	6	18	45	71	29	5	53	39	145	245
Mean	.056	.014	.014	.169	.563	.113	.099	.085	.254	.634	1.000	.408	.070	.746	.549	2.042	3.408
Median	0	0	0	0	1	0	0	0	0	0	1	0	0	1	0	2	3
Minimum	0	0	0	0	0	0	0	0	0	0	0	0	0	0	0	0	0
Maximum	1	1	1	1	2	1	1	1	2	3	4	2	1	2	3	5	7
Variance	.054	.014	.014	.142	.335	.101	.090	.078	.249	.578	.886	.302	.066	.392	.537	1.612	2.559
Standard Deviation	.232	.119	.119	.377	.579	.318	.300	.280	.499	.760	.941	.550	.258	.626	.733	1.270	1.600

4.2 Testing the Distribution of Data for Frequency of Occurrences Over Time

Simple histograms were constructed to demonstrate the distribution of the entire data set (1950 to 2020) for each study area. The display of both distributions confirmed the non-normal shape (Figure 4.2.1 and Figure 4.2.2). The frequency of tropical cyclones within this dataset was not normally distributed, thus, and non-parametric techniques were required for analysis of this dataset. Additionally, a time series was provided to display the number of tropical cyclones per year for the entire study period and each study area (Figure 4.2.3 and Figure 4.2.4).

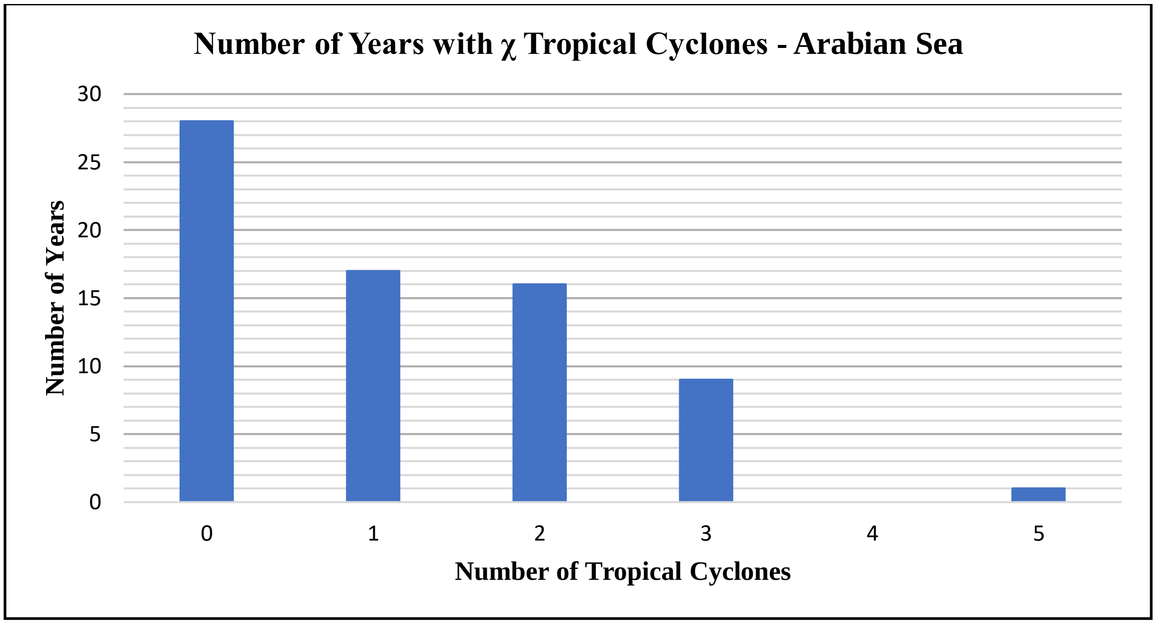

Figure 4.2.1 Arabian Sea Histogram. A histogram of the Arabian Sea exhibiting an abnormal distribution using the entire study period of 1950 to 2020.

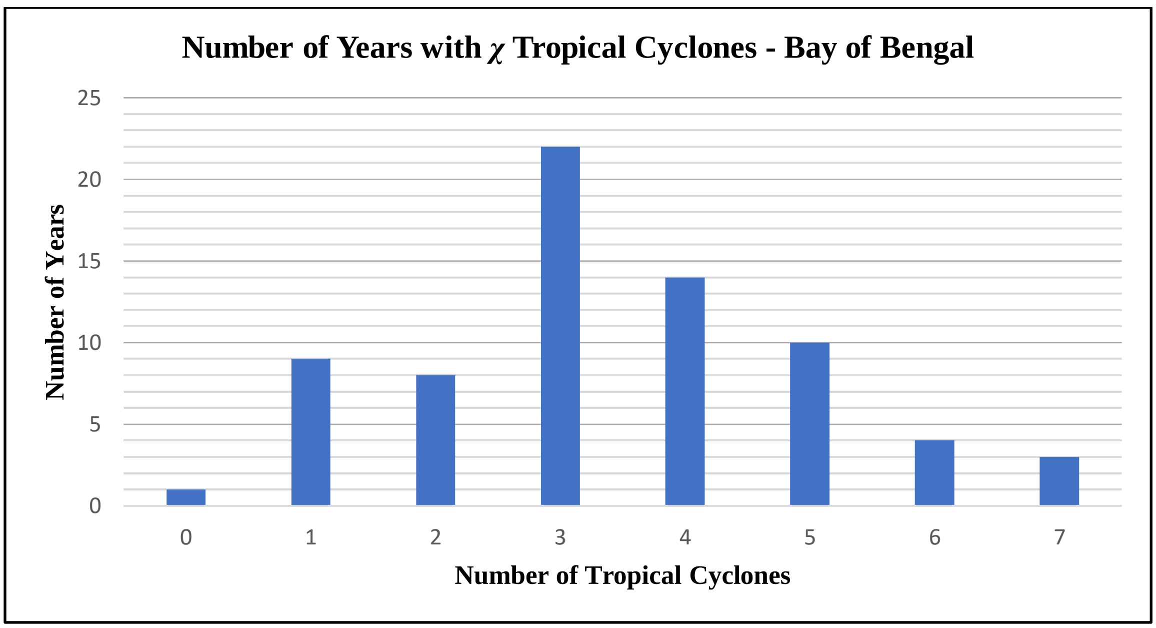

Figure 4.2.2 Bay of Bengal Histogram. A histogram of the Bay of Bengal exhibiting an abnormal distrubiton using the entire study period of 1950 to 2020.

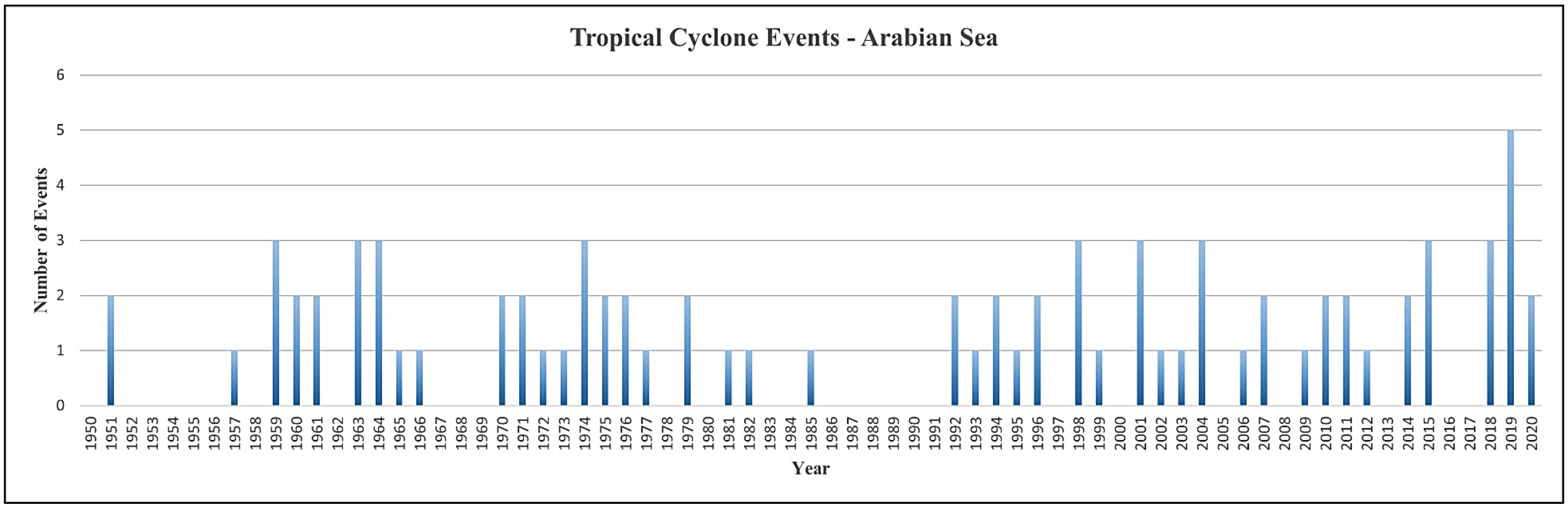

Figure 4.2.3 Tropical Cyclone Events within the Arabian Sea. Time series showing the distribution of tropical cyclone events from 1950 to 2020 in the Arabian Sea.

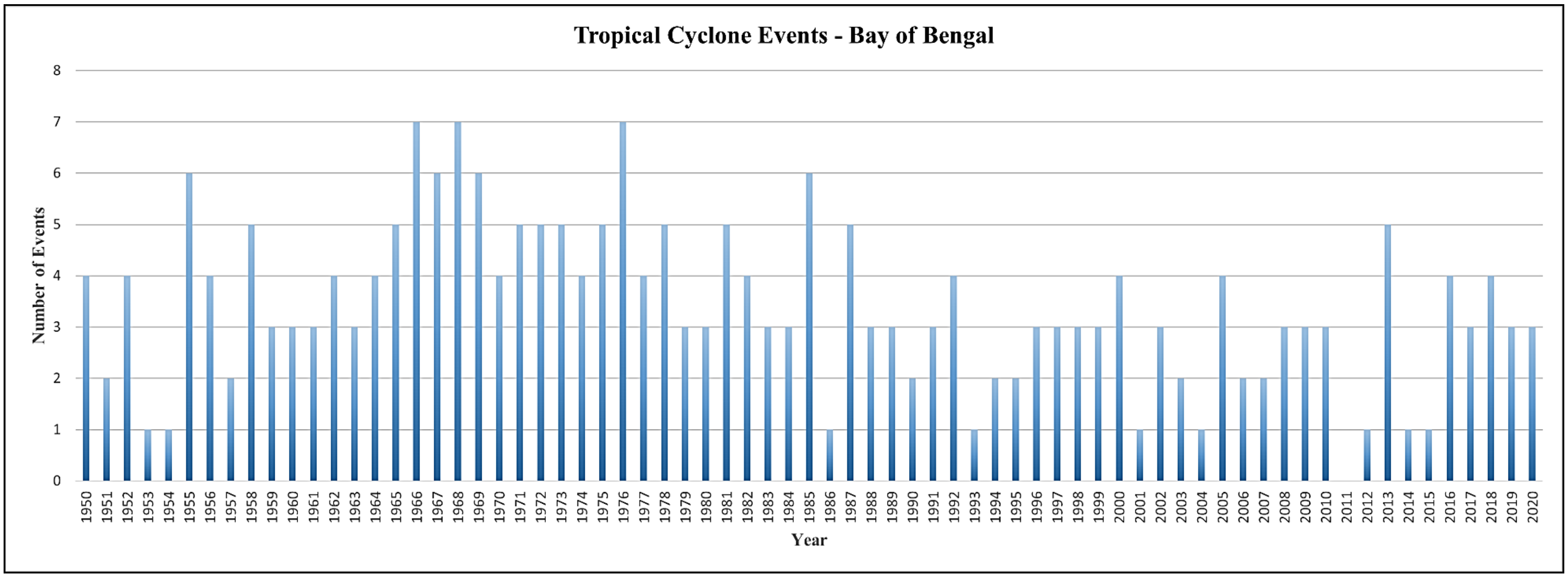

Figure 4.2.4 Tropical Cyclone Events within the Bay of Bengal. Time series showing the distribution of tropical cyclone events from 1950 to 2020 in the Bay of Bengal.

4.3 Trend Analysis for Temporal Frequency of Occurrences

The Cox-Stuart analysis found no statistically significant trend within the Arabian Sea using an alpha value of $\alpha = 0.025$ in a one-tail test for the entire study period of 1950 to 2020. Therefore, the analysis failed to reject H_0. This was true for all monthly, seasonal, and annual calculations (Table 4.3.1). The Cox-Stuart analysis for the Bay of Bengal found that August and September showed statistically significant trends, as well as for the Southwest monsoon season and annually with p-values of 0.021, 0.015, 0.002, and 0.003, respectively (Table 4.3.2). The analysis rejected H_0 for August, September, the Southwest Monsoon season, and annually for the Bay of Bengal trend results.

4.3.1 Regression Analysis of Cox-Stuart Trend

For the months, seasons, and annual calculations that were found to have a statistically significant trend, a time series was plotted with the number of tropical cyclone occurrences per year to retrieve a regression slope and p-value using the software statistical program JMP (Figures 4.3.1-4.3.4). Excel was used to graph each regression analysis. The regression slopes and respective p-values may be found in Table 4.3.3.

Table 4.3.1 Arabian Sea Cox-Stuart Analysis for Trend. Cox-Stuart analysis for trend in the Arabian Sea from 1950 to 2020. H_0, there is no significant trend; H_A (bolded), there is a significant trend.

Arabian Sea																	
	J	*F*	*M*	*A*	*M*	*J*	*J*	*A*	*S*	*O*	*N*	*D*	*JF*	*MAM*	*JJAS*	*OND*	*ANN*
Number of Pairs	0	0	0	2	12	12	0	0	7	12	11	6	0	12	18	18	22
Number of Positive Pairs	0	0	0	2	6	5	0	0	3	4	5	3	0	7	8	7	11
Number of Negative Pairs	0	0	0	0	6	7	0	0	4	8	6	3	0	5	10	11	11
p-value	0	0	0	0.275	0.222	0.211	0	0	0.285	0.146	0.234	0.31	0	0.211	0.180	0.145	0.141

Table 4.3.2 Bay of Bengal Cox-Stuart Analysis for Trend. Cox-Stuart analysis for trend in the Bay of Bengal from 1950 to 2020. H_0, there is no significant trend; H_A (bolded), there is a significant trend.

Bay of Bengal																	
	J	*F*	*M*	*A*	*M*	*J*	*J*	*A*	*S*	*O*	*N*	*D*	*JF*	*MAM*	*JJAS*	*OND*	*ANN*
Number of Pairs	4	1	1	19	19	8	7	6	13	19	23	13	5	20	21	29	27
Number of Positive Pairs	1	0	1	13	13	6	5	6	11	13	14	9	1	13	18	19	22
Number of Negative Pairs	3	1	0	6	6	2	2	0	2	6	9	4	4	7	3	10	5
p-value	0.28	0.525	0.525	0.075	0.075	0.137	0.189	**0.021**	**0.015**	0.072	0.122	0.11	0.18	0.098	**0.002**	0.121	**0.003**

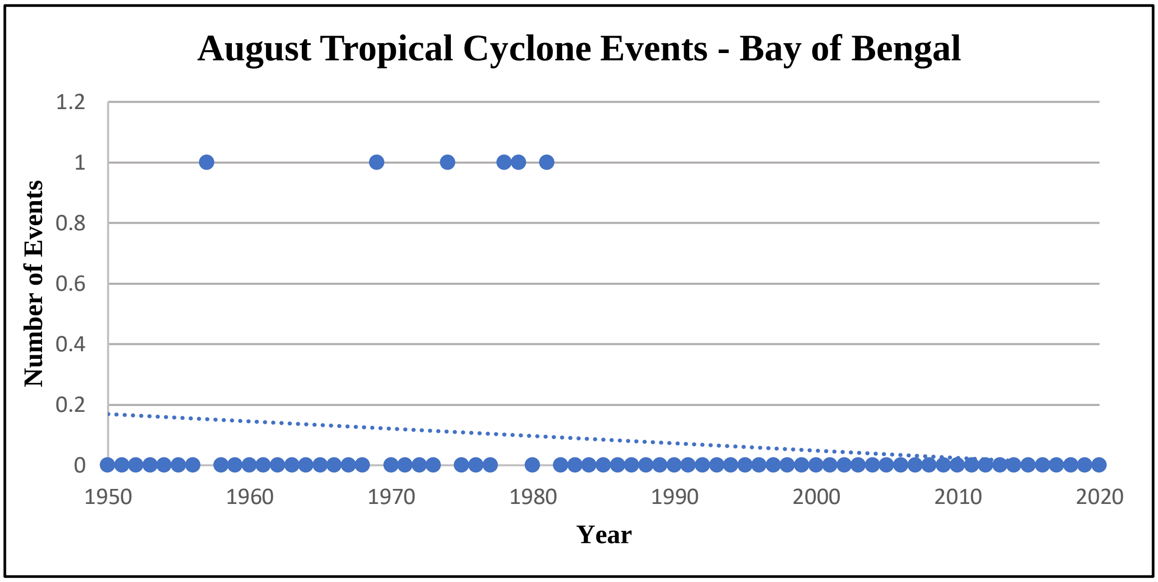

Figure 4.3.1 Regression Analysis of August Tropical Cyclones within the Bay of Bengal (1950 to 2020). By rejecting H_0, there was a significant trend via the Cox-Stuart Trend analysis, with a regression slope of -0.002 and a p-value of 0.138.

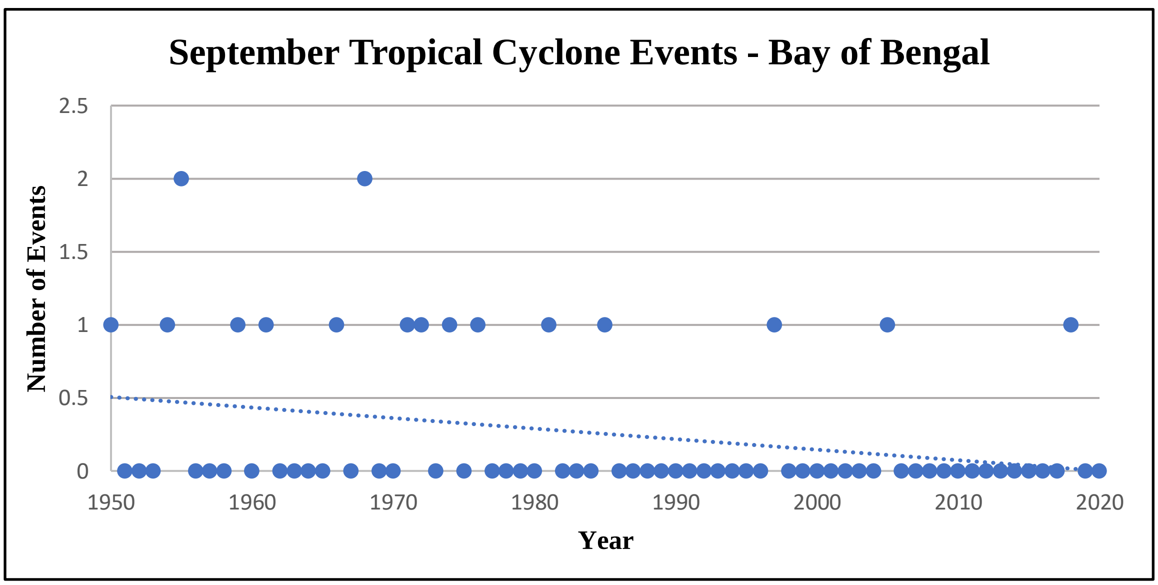

Figure 4.3.2 Regression Analysis of September Tropical Cyclones within the Bay of Bengal (1950 to 2020). By rejecting H_0, there was a significant trend via the Cox-Stuart Trend analysis, with a regression slope of -0.007 and a p-value of 0.012.

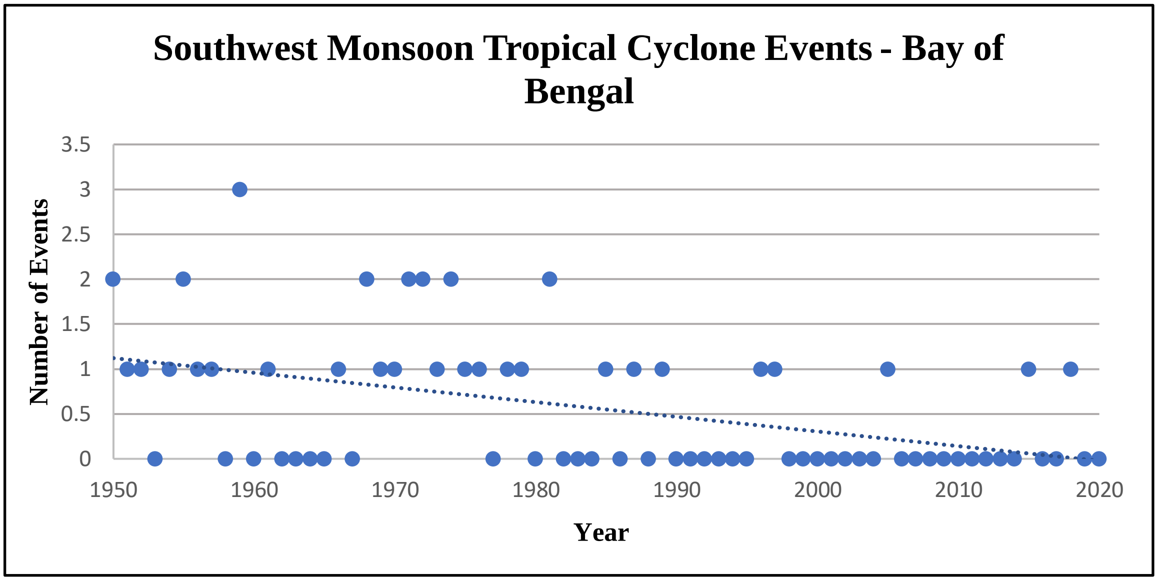

Figure 4.3.3 Regression Analysis of the Southwest Monsoon Season Tropical Cyclones within the Bay of Bengal (1950 to 2020). By rejecting H_0, there was a significant trend via the Cox-Stuart Trend analysis, with a regression slope of -0.016 and a p-value of <0.0001.

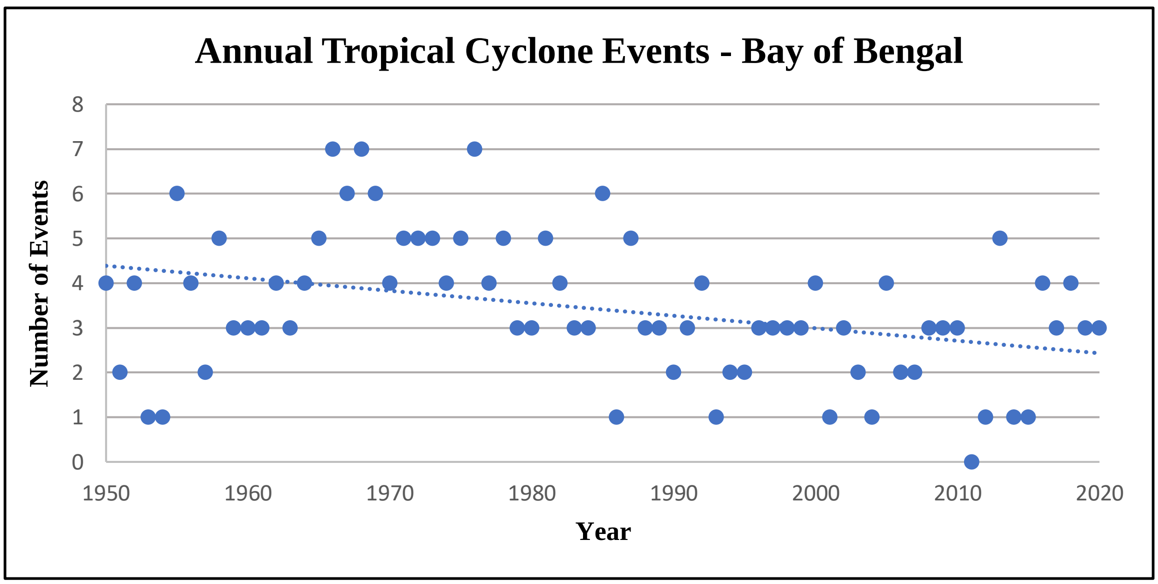

Figure 4.3.4 Regression Analysis of Annual Tropical Cyclones within the Bay of Bengal (1950 to 2020). By rejecting H_0, there was a significant trend via the Cox-Stuart Trend analysis, with a regression slope of -0.028 and a p-value of 0.002.

Table 4.3.3 Regression Analysis. Regression analysis values of Cox-Stuart statistically significant trends within the Bay of Bengal from 1950 to 2020.

	August	*September*	*Southwest Monsoon*	*Annual*
slope	-0.002	-0.007	-0.016	-0.028
p-value	0.138	**0.012**	**<0.0001**	**0.002**

4.4 Chi-Square Goodness of Fit Test

The Chi-Square Goodness of Fit test found statistically significant differences from the expected distribution during the month of June, the post-monsoon season, and annually for ENSO tropical cyclone frequencies in the Arabian Sea using two degrees of freedom. The month of June, the post-monsoon season, and annual did not follow the expected distribution pattern when using $\alpha = 0.025$, and therefore, rejected H_0 (Table 4.4.1). The IOD tropical cyclone frequencies within the Arabian Sea were found to not follow the expected distribution annually also rejected H_0 (Table 4.4.2). The distributions that do not follow the expected pattern of tropical cyclones suggested a dependent relationship between the IOD, ENSO, and tropical cyclones occurrences.

Within the Bay of Bengal, January, April, May, July, the winter season, the pre-monsoon season, and annually, indicated that tropical cyclone frequencies did not follow the expected distribution for ENSO tropical cyclone frequencies and therefore, rejected H_0 with an alpha value of $\alpha = 0.025$ using two degrees of freedom (Table 4.4.3). The IOD tropical cyclone frequencies within the Bay of Bengal did not follow the distribution for April, September, the winter season, the post-monsoon season, and annually, and also rejected H_0 (Table 4.4.4). The Bay of Bengal Chi-Square Goodness of Fit test resulted in more deviation from expected tropical cyclone frequencies than the Arabian Sea, which may demonstrate more frequency dependence upon the IOD and ENSO phases.

Table 4.4.1 Chi-Square Goodness of Fit Test – ENSO and the Arabian Sea. Chi-Square Goodness of Fit test used the transformed ENSO index and Arabian Sea tropical cyclone frequencies from 1950 to 2020. H_0, observations followed the expected distribution of tropical cyclones; H_A, observations did not follow the expected distribution of tropical cyclones.

	Chi² -1	***Chi² 0***	***Chi² 1***	***Sum of Chi²***	***DF***	***α = 0.025***
J	0	0	0	0	2	H_0
F	0	0.054	0	0	2	H_0
M	0	0.520	0	0	2	H_0
A	0.670	0.265	0.113	0.915	2	H_0
M	0.022	0	1.014	1.175	2	H_0
J	0.310	0.054	8.834	9.318	2	$\mathbf{H_A}$
J	0	0.520	0	0	2	H_0
A	2.945	0.265	0.113	3.733	2	H_0
S	2.070	0	1.860	4.109	2	H_0
O	0.068	0.054	0.665	0.816	2	H_0
N	0.544	0.520	5.656	7.331	2	H_0
D	0.373	0.265	2.368	5.360	2	H_0
JF	0	0	0	0	2	H_0
MAM	0.054	0.028	1.127	1.209	2	H_0
JJAS	0.520	0.048	2.238	2.806	2	H_0
OND	0.265	1.535	6.055	7.854	2	$\mathbf{H_A}$
ANN	0.031	4.501	52.218	56.749	2	$\mathbf{H_A}$

Table 4.4.2 Chi-Square Goodness of Fit Test – IOD and the Arabian Sea. Chi-Square Goodness of Fit test using the transformed IOD index and Arabian Sea tropical cyclone frequencies from 1950 to 2020. H_0, observations followed the expected distribution of tropical cyclones; H_A, observations did not follow the expected distribution of tropical cyclones.

	Chi² -1	***Chi² 0***	***Chi² 1***	***Sum of Chi²***	***DF***	***α = 0.025***
J	0	0	0	0	2	H_0
F	0	0	0	0	2	H_0
M	0	0	0	0	2	H_0
A	2.663	0.264	0	2.927	2	H_0
M	0.001	0.276	0.006	0.282	2	H_0
J	0.310	0.087	$2.55*10^{-6}$	0.397	2	H_0
J	0	0	0	0	2	H_0
A	2.416	0.563	$1.70*10^{-7}$	2.979	2	H_0
S	0.630	0.034	$8.22*10^{-9}$	0.664	2	H_0
O	0.210	2.035	0.010	2.255	2	H_0
N	0.075	0.146	$1.53*10^{-8}$	0.221	2	H_0
D	0.338	0.086	$1.22*10^{-5}$	0.424	2	H_0
JF	0	0	0	0	2	H_0
MAM	4.650	0.214	0.002	4.866	2	H_0
JJAS	0.412	0.110	$3.92*10^{-6}$	0.523	2	H_0
OND	3.633	2.802	0.004	6.439	2	H_0
ANN	8.627	5.553	0.002	14.182	2	$\mathbf{H_A}$

Table 4.4.3 Chi-Square Goodness of Fit Test – ENSO and the Bay of Bengal. Chi-Square Goodness of Fit test using the transformed ENSO index and Bay of Bengal tropical cyclone frequencies from 1950 to 2020. H_0, observations followed the expected distribution of tropical cyclones; H_A, observations did not follow the expected distribution of tropical cyclones.

	Chi² -1	***Chi² 0***	***Chi² 1***	***Sum of Chi²***	***DF***	***α = 0.025***
J	1.240	0.479	6.200	7.918	2	**H_A**
F	2.663	0.634	0.141	3.438	2	H_0
M	2.663	0.648	0.127	3.438	2	H_0
A	0.183	0.304	7.989	8.476	2	**H_A**
M	0.260	0.617	14.654	15.530	2	**H_A**
J	1.283	0.714	1.296	3.293	2	H_0
J	0.211	0.694	9.806	10.711	2	**H_A**
A	1.268	0.001	2.593	3.861	2	H_0
S	0.330	0.012	0.466	0.807	2	H_0
O	0.007	0.845	2.751	3.602	2	H_0
N	0.640	1.633	0.563	2.836	2	H_0
D	1.010	0.218	3.876	5.104	2	H_0
JF	0.086	1.234	6.393	7.712	2	**H_A**
MAM	0.075	1.313	21.510	22.898	2	**H_A**
JJAS	0.012	0.898	4.827	5.737	2	H_0
OND	$4.05*10^{-6}$	2.335	4.992	7.327	2	H_0
ANN	3.837	25.694	201.134	230.664	2	**H_A**

Table 4.4.4 Chi-Square Goodness of Fit Test – IOD and the Bay of Bengal. Chi-Square Goodness of Fit test using the transformed IOD index and Bay of Bengal tropical cyclone frequencies from 1950 to 2020. H_0, observations followed the expected distribution of tropical cyclones; H_A, observations did not follow the expected distribution of tropical cyclones.

	Chi² -1	***Chi² 0***	***Chi² 1***	***Sum of Chi²***	***DF***	***α = 0.025***
J	0.394	0.003	0.479	0.877	2	H_0
F	0.127	0.066	0.099	0.291	2	H_0
M	0.099	0.048	0.099	0.246	2	H_0
A	0.092	0.390	7.989	8.470	2	**H_A**
M	3.975	0.940	0.226	5.141	2	H_0
J	0.113	0.094	1.127	1.334	2	H_0
J	0.678	0.226	0.028	0.932	2	H_0
A	1.701	0.043	1.183	2.927	2	H_0
S	5.272	4.340	0.302	9.913	2	**H_A**
O	0.271	0.030	0.143	0.444	2	H_0
N	0.111	1.280	4.083	5.474	2	H_0
D	0.082	0.003	0.246	0.331	2	H_0
JF	0.282	0.012	0.522	0.815	2	**H_A**
MAM	22.217	4.245	3.043	29.505	2	H_0
JJAS	9.997	3.478	0.044	13.520	2	H_0
OND	0.713	0.006	0.958	1.677	2	**H_A**
ANN	32.420	8.375	7.046	47.841	2	**H_A**

4.5 Chi-Square Test of Independence

The Chi-Square Test of Independence examined the relationship between ENSO and the IOD phases combined, with the null hypothesis that ENSO and the IOD are independent of one another, and the alternative hypothesis that they do not have an independent relationship from one another. Both study areas exhibited the same phase of the IOD and ENSO, respective to the month and year. The months of May, September, October, and November, as well as the Southwest monsoon season, and post-monsoon season all rejected H_0 when using $\alpha = 0.005$ with two degrees of freedom, indicating that during these periods, ENSO and IOD did not show complete independence (Table 4.5). This suggests that throughout the study period (1950 to 2020), the above-mentioned months and seasons may demonstrate some dependency within the IOD and ENSO dynamics through the Arabian Sea and the Bay of Bengal.

Table 4.5 Chi-Square Test of Independence. Chi-Square Test of Independence using the transformed ENSO and IOD indices, and phase frequencies from 1950 to 2020. H_0, ENSO and IOD were independent of one another; H_A, ENSO and IOD were not independent of one another.

	Sum of Chi²	***DF***	***α = 0.005***
J	9.724	2	H_0
F	1.471	2	H_0
M	7.199	2	H_0
A	8.020	2	H_0
M	48.163	2	$\mathbf{H_A}$
J	4.278	2	H_0
J	8.345	2	H_0
A	12.167	2	H_0
S	26.568	2	$\mathbf{H_A}$
O	22.895	2	$\mathbf{H_A}$
N	16.269	2	$\mathbf{H_A}$
D	12.953	2	H_0
JF	0.997	2	H_0
MAM	9.637	2	H_0
JJAS	16.295	2	$\mathbf{H_A}$
OND	25.075	2	$\mathbf{H_A}$
ANN	4.373	2	H_0

5. DISCUSSION

5.1 Descriptive Statistics: Temporal Changes in Frequency of Occurrences

The Arabian Sea has not produced a tropical cyclone in either January, February, March, or July since 1950. When comparing the means of all monthly, seasonal, and annual statistics in the Arabian Sea, it was found that about one tropical cyclone is produced per year with frequency progressively increasing each season. It should also be noted that within the Arabian Sea, the post-monsoon season had the highest seasonal mean of 0.535, but the standard deviation was also highest at 0.693. Within the Bay of Bengal, the months of January, February, and March had the lowest totals (less than five) of tropical cyclones throughout the 71 years, and June, July, and August also exhibited lower frequencies of less than 10 tropical cyclones each. May and November have the most frequent tropical cyclones (median of one), with November exhibiting an average of one tropical cyclone per year within the Bay of Bengal. However, the minimum (zero) and maximum (seven) tropical cyclones annually raises concern regarding the technology or lack thereof to record tropical cyclones, as well as the accuracy and precision of equipment that may or may not classify a tropical storm within the “cyclone” category. Satellite imagery, the most used technology to collect such data did not become more widely utilized and accurate until the late 1960’s.

5.2 Testing the Distribution of Data

The results from the Arabian Sea histogram established the abnormal or non-bell curve distribution of tropical cyclone frequencies throughout the entire time period (1950 to 2020). The Bay of Bengal did present a normal distribution curve, but to compare and examine both study areas with the same quantitative analyses requires non-parametric tests. Additionally, neither of the time series displayed an obvious increase or decrease of tropical cyclone frequencies. These results determined the use of non-parametric tests, tests that do not assume a normal distribution. The Cox-Stuart test, Chi-Square Goodness of Fit test, and Chi-Square Test of Independence are all non-parametric and provide robust results.

5.3 Trend Analysis for Temporal Frequency of Occurrences

The number of pairs or differences found using the Cox-Stuart trend analysis in the Arabian Sea showed no significant trends for any month, season, or annually. The Bay of Bengal, however, presented four significant temporal trends during August, September, the pre-monsoon season, and annually, all of which displayed a steep decrease in frequency or number of positive pairs. It should be noted that August and September did occur during the defined pre-monsoon season and therefore, all three having significant trends is reasonable. The annual number of positive pairs could indicate a decrease in frequency trend, which is also supported by the high variance (2.559) in the descriptive statistics. The Cox-Stuart trend test does not directly imply an increase or decrease in frequency temporally, but instead displays a significant trend in any direction and strength.

5.3.1 Regression Analysis of Cox-Stuart Trend

The regression analysis of the statistically significant Cox-Stuart trends (August, September, pre-monsoon, and annually) within the Bay of Bengal were all weak (slope < 0.020) and negative, indicating a small decrease in temporal tropical cyclone frequency (1950 to 2020). When viewing the regression results, it became apparent that the Cox-Stuart non-parametric trend was productive. Creating a regression for each significant trend and calculating the associated p-value for each month confirmed that the trend was not by chance, and therefore indicated a difference in tropical cyclone frequency over time.

5.4 Chi-Square Goodness of Fit Test

The Chi-Square Goodness of Fit test examined if the observed tropical cyclone frequency followed the expected pattern for months, seasons, and annual trends. The results for the Arabian Sea suggested that frequency of occurrences of tropical cyclones during June and the post-monsoon season were dependent upon the ENSO phase but not the phase of the IOD. Annual tropical cyclone occurrences were influenced by both the ENSO phase and the IOD phase. Within the Arabian Sea, only four of the 34 tested durations (12 months, 4 seasons, annual * 2 indices) rejected the null hypothesis, and therefore, it was concluded that both the ENSO and IOD phase had little to no impact or influence within the study area.

The Bay of Bengal results were vastly different. The results from the months of January, May, July, and the pre-monsoon season suggested that tropical cyclone occurrences were influenced by the phase of ENSO, while September and the post-monsoon season were only influenced by the IOD phase within the Bay of Bengal. During April, the winter monsoon, and annually, both ENSO and the IOD phase influenced the occurrence of tropical cyclones, within this 71-year study. Of the 34 analyzed durations, 12 did not fit the expected distribution within the Bay of Bengal. This demonstrated that the ENSO and IOD phases had a slight impact during specific time intervals.

The overall results collected from the Chi-Square Goodness of Fit test determined that the Arabian Sea was influenced little to none by neither the IOD or ENSO phases, but the Bay of Bengal did exhibit several specific months or seasons when the phase of the IOD and ENSO do have a slight influence on tropical cyclone occurrence.

5.5 Chi-Square Test of Independence

The relationship between the ENSO and IOD phases was examined through the Chi-Square Test of Independence and found that May, September, October, November, the Southwest monsoon season, and the post-monsoon season all displayed patterns of dependency, or not being completely independent of one another. November and the Southwest monsoon season particularly only displayed this when using an alpha of 0.005 but failed to display dependency with increased alpha values. However, six of the 17 tested durations had a significant lack of independence that was not likely due to chance. Additionally, the most common indices value pairs (IOD, ENSO) that occurred throughout the 71 years were (-1, 0) and (0, -1), with 15 of the 17. This means that the most common IOD-ENSO phase pairs were IOD cool anomalies with neutral ENSO temperatures, and neutral IOD temperatures, and warm ENSO anomalies. Furthermore, the least common IOD-ENSO phase pairs were (-1, 1) and (1, -1) with 15 of the 17, or IOD cool anomalies with ENSO cool anomalies, and warm IOD anomalies with warm ENSO anomalies. The Chi-Square test of independence exhibited results suggesting that the IOD and ENSO were not entirely independent of one another throughout different temporal durations, based off the index data utilized within this study. Reasons for this result could be explored in a future study.

6. CONCLUSION

The objective of this study was to determine a temporal trend of tropical cyclone frequency within the Arabian Sea and Bay of Bengal from 1950 to 2020, to establish if the observed tropical cyclone frequencies aligned with the expected distributions, and lastly to examine the relationship between phases of the Indian Ocean Dipole (IOD) and El Niño Southern Oscillation (ENSO). This was done by conducting non-parametric quantitative analyses using tropical cyclone frequencies, IOD and ENSO indices. Findings from these analyses were as follows:

1. The descriptive statistics of each study area were obtained with the mean, median, minimum, maximum, variance, and the standard deviation using all tropical cyclone occurrences within each time frame (monthly, seasonal, and annual) for the entire period of research (71 years). The means, maximums, and standard deviations within the Bay of Bengal were greater than the Arabian Sea calculations in every time frame. Viewing the ranges of frequency and standard deviations led to the hypothesis of an abnormal distribution of data.
2. Testing the distribution of data was conducted by creating a simple histogram of tropical cyclone frequency, allowing the shape of the distribution to be easily seen and referenced when determining the appropriate tests for the dataset. The results for each histogram concluded that the dataset was not normally shaped, and therefore, the more appropriate tests would be from non-parametric statistical analyses.

3. A Cox-Stuart trend analysis was conducted to determine if there was a significant temporal trend in the data from 1950 to 2020. The test found no significant trends in the Arabian Sea; however, the trend analysis found statistically significant trends in the Bay of Bengal for August, September, the Southwest monsoon season, and annually. A regression analysis for each significant trend indicated slight decreasing trends in tropical cyclone frequencies.
4. The Chi-Square Goodness of Fit test compared observed tropical cyclone frequencies within each study area to the expected frequencies to determine if the observed frequencies were impacted by the IOD or ENSO phases using transformed indices. Within the Arabian Sea, June and the post-monsoon season were influenced by the ENSO phase, while annual frequencies were influenced by both the IOD and ENSO phase. Within the Bay of Bengal, January, May, July, and pre-monsoon frequencies were impacted by the phase of ENSO. September and the post-monsoon season exhibited influence from only the IOD phase. Lastly, April, the winter season, and annual tropical cyclone frequencies were impacted by both the IOD and ENSO phase. Overall, the phase of the IOD had little to no impact on Arabian Sea frequencies, and slight impact within the Bay of Bengal.
5. The last non-parametric test was the Chi-Square Test of Independence which examined the relationship between the IOD and ENSO phases. It was determined that the IOD and ENSO do not exhibit complete independence from one another during the months of May, September, October, and

November, as well as the Southwest monsoon season, and post-monsoon season.

The results from this research are supported by previous research, however, tropical cyclone frequency research, specifically, within the study areas of the Arabian Sea and Bay of Bengal is very limited and therefore more research needs to be contributed using these study areas.

Limitations and errors within this research include utilization of secondary data and lack of readily available accurate technology. Satellites were not available for widespread use until the late 1960’s so measurements and classifications were based upon ship and land measurements, potentially skewing the dataset. When looking to the future, researchers will use improved technologies and new datasets to hopefully broaden the scope of tropical cyclone knowledge within the Northern Indian Ocean. There is a need for such research as climate change is rapidly shifting the global, regional, and local patterns, and populations are experiencing the associated hazards.

REFERENCES

Ali A (1979) Storm surges in the Bay of Bengal and some related problems. Ph.D. Thesis, University of Reading, England.

Ankur, K., N. K. R. Busireddy, K. K. Osuri, and D. Niyogi. 2020. On the relationship between intensity changes and rainfall distribution in tropical cyclones over the North Indian Ocean. *International Journal of Climatology* 40 (4):2015–2025. http://rmets.onlinelibrary.wiley.com/doi/abs/10.1002/joc.6315

Arabian Sea. 2018. *Funk & Wagnalls New World Encyclopedia* :1; http://libproxy.txstate.edu/login?url=https://search.ebscohost.com/login.aspx?direct=true&db=funk&AN=ar127900&site=eds-live&scope=site

Bay of Bengal. *WorldAtlas*. https://www.worldatlas.com/bays/bay-of-bengal.html

Bay of Bengal. 2018. *Funk & Wagnalls New World Encyclopedia* :1; http://libproxy.txstate.edu/login?url=https://search.ebscohost.com/login.aspx?direct=true&db=funk&AN=be071000&site=eds-live&scope=site

Bhatia, K., G. Vecchi, H. Murakami, S. Underwood, and J. Kossin. 2018. Projected Response of Tropical Cyclone Intensity and Intensification in a Global Climate Model. *Journal of Climate* 31 (20):8281–8303.

Bjerknes, J. 1966. A possible response of the atmospheric Hadley circulation to equatorial anomalies of ocean temperature. *Tellus* 18 (4):820–829. https://onlinelibrary.wiley.com/doi/abs/10.1111/j.2153-3490.1966.tb00303.x

Chowdhury, R. R., S. P. Kumar, J. Narvekar, and A. Chakraborty. 2020. Back-to-Back Occurrence of Tropical Cyclones in the Arabian Sea During October–November 2015: Causes and Responses. *Journal of Geophysical Research: Oceans* 125 (6):e2019JC015836. http://agupubs.onlinelibrary.wiley.com/doi/abs/10.1029/2019JC015836

Clark, C. O., P. J. Webster, and J. E. Cole. 2003. Interdecadal Variability of the Relationship between the Indian Ocean Zonal Mode and East African Coastal Rainfall Anomalies. *Journal of Climate* 16 (3):548–554. https://journals.ametsoc.org/view/journals/clim/16/3/1520-0442_2003_016_0548_ivotrb_2.0.co_2.xml

Collins, J. M., and K. Walsh eds. 2017. *Hurricanes and Climate Change*. Cham: Springer International Publishing.

Cushman, G. 2003. The presidential symposium on the history of the atmospheric sciences: people, discoveries, and technologies. *1.1 who discovered the El Niño-southern oscillation? (2003 - annual2003_historysymp)*. https://ams.confex.com/ams/annual2003/techprogram/paper_58909.htm

Daniel, W. W. 1978. *Applied non-parametric statistics*. Boston, MA: Houghton Mifflin.

Du, Y., and S.-P. Xie. 2008. Role of atmospheric adjustments in the tropical Indian Ocean warming during the 20th century in climate models. *Geophysical Research Letters* 35 (8). https://agupubs.onlinelibrary.wiley.com/doi/abs/10.1029/2008GL033631

El Niño and La Niña. 2021. *El Niño & La Niña (El Niño-Southern Oscillation) | NOAA Climate.gov*. https://www.climate.gov/enso.

Esri. "Charted Territory" [basemap]. Scale Not Given. "Charted Territory Map". May 25, 2018. https://learngis2.maps.arcgis.com/home/webmap/viewer.html?webmap=5272595f6ca24546abcf502ca2c5b7ed.

Fitchett, J. 2018. Recent emergence of CAT5 tropical cyclones in the South Indian Ocean. *South African Journal of Science* 114 (11/12):83–88.

Glossary of NHC Terms. https://www.nhc.noaa.gov/aboutgloss.shtml

Halpert, M., Barnston, A., L'Heureux, M., and Becker, E. 2016. El Niño and La Niña: Frequently asked questions. *National Oceanic and Atmospheric Administration.* https://www.climate.gov/news-features/understanding-climate/el-ni%C3%B1o-and-la-ni%C3%B1a-frequently-asked-questions

Henderson-Sellers A., Zhang H., Berz G., Emanuel K., Gray W., Landsea C., Holland G., Lighthill J., Shieh S-L., Webster P., and McGuffie K. 1998. Tropical Cyclones and Global Climate Change : A Post-IPCC Assessment. *Bulletin of the American Meteorological Society* 79 (1):19–38.

Hyndman, D. W., and D. W. Hyndman. 2017. *Natural hazards and disasters* 5th ed. Boston, MA: Cengage Learning.

India Meteorological Department. 2020. Seasonal Frequency of Cyclone and above. https://rsmcnewdelhi.imd.gov.in/frequency-of-formation-of-cyclone.php.

Intergovernmental Panel on Climate Change (IPCC). 2013. IPCC Fifth Assessment Report (AR5) Observed Climate Change Impacts Database, Version 2.01. https://doi.org/10.7927/H4FT8J0X

Intergovernmental Panel on Climate Change. 2021. Summary for Policymakers. In: Climate Change 2021: The Physical Science Basis. Contribution of Working Group I to the Sixth Assessment Report of the Intergovernmental Panel on Climate Change MassonDelmotte, V., P. Zhai, A. Pirani, S. L. Connors, C. Péan, S. Berger, N. Caud, Y. Chen, L. Goldfarb, M. I. Gomis, M. Huang, K. Leitzell, E. Lonnoy, J. B. R. Matthews, T. K. Maycock, T. Waterfield, O. Yelekçi, R. Yu and B. Zhou (eds.). Cambridge University Press. In Press.

Johnson, N. 2020. Meet ENSO's neighbor, the Indian Ocean Dipole. *Meet ENSO's neighbor, the Indian Ocean Dipole | NOAA Climate.gov*. https://www.climate.gov/news-features/blogs/enso/meet-enso%E2%80%99s-neighbor-indian-ocean-dipole.

Klein, S. A., B. J. Soden, and N.-C. Lau. 1999. Remote Sea Surface Temperature Variations during ENSO: Evidence for a Tropical Atmospheric Bridge. *Journal of Climate* 12 (4):917–932. https://journals.ametsoc.org/view/journals/clim/12/4/1520-0442_1999_012_0917_rsstvd_2.0.co_2.xml

Knutson, T., S. J. Camargo, J. C. L. Chan, K. Emanuel, C.-H. Ho, J. Kossin, M. Mohapatra, M. Satoh, M. Sugi, K. Walsh, and L. Wu. 2020. Tropical Cyclones and Climate Change Assessment: Part II: Projected Response to Anthropogenic Warming. *Bulletin of the American Meteorological Society* 101 (3):E303–E322. https://journals.ametsoc.org/view/journals/bams/101/3/bams-d-18-0194.1.xml

Kossin, J. P., T. L. Olander, and K. R. Knapp. 2013. Trend analysis with a new global record of tropical cyclone intensity. *Journal of Climate* 26 (24):9960–9976.

Lee, C.-Y., M. K. Tippett, S. J. Camargo, and A. H. Sobel. 2015. Probabilistic Multiple Linear Regression Modeling for Tropical Cyclone Intensity. *Monthly Weather Review* 143 (3):933–954.

L'Heureux, M. 2014. What is the El Niño-Southern Oscillation (ENSO) in a nutshell? *National Oceanic and Atmospheric Administratio.*https://www.climate.gov/news-features/blogs/enso/what-el-ni%C3%B1o%E2%80%93southern-oscillation-enso-nutshell

McAdie, C. J., Landsea, C. W., Neumann, C. J., David, J. E., Blake, E. S., and G. R. Hammer. 2009. *Tropical cyclones of the North Atlantic Ocean, 1851-2006 Historical Climatology Series* 6-2. Asheville, NC: National Centers for Environmental Information, NESDIS, NOAA, U.S. Department of Commerce.

Mittal, R., M. Tewari, C. Radhakrishnan, P. Ray, T. Singh, and A. K. Nickerson. 2019. Response of tropical cyclone Phailin (2013) in the Bay of Bengal to climate perturbations. *Climate Dynamics* 53 (3–4):2013–2030.

Murakami, H., R. Mizuta, and E. Shindo. 2012. Future changes in tropical cyclone activity projected by multi-physics and multi-SST ensemble experiments using the 60-km-mesh MRI-AGCM. *Climate Dynamics* 39 (9):2569–2584. https://doi.org/10.1007/s00382-011-1223-x

Needham, H. F., B. D. Keim, and D. Sathiaraj. 2015. A review of tropical cyclone-generated storm surges: Global data sources, observations, and impacts. *Reviews of Geophysics* 53 (2):545–591. https://agupubs.onlinelibrary.wiley.com/doi/abs/10.1002/2014RG000477

National Oceanic and Atmospheric Administration. 2022. Climate Timeseries. https://psl.noaa.gov/gcos_wgsp/Timeseries/

Paul, B. K., and H. Rashid. 2017. Tropical Cyclones and Storm Surges. In *Climatic hazards in coastal Bangladesh: non-structural and structural solutions*, 35–81. Amsterdam: Butterworth-Heinemann, an imprint of Elsevier https://www.sciencedirect.com/science/article/pii/B9780128052761000028

Rafiq, L., T. Blaschke, and S. Tajbar. 2015. Arabian Sea cyclone: Structure analysis using satellite data. *Advances in Space Research* 56 (10):2235–2247. https://www.sciencedirect.com/science/article/pii/S027311771500558X

Saji, N. H., B. N. Goswami, P. N. Vinayachandran, and T. Yamagata. 1999. A dipole mode in the tropical Indian Ocean. *Nature* 401 (6751):360–363. https://www.nature.com/articles/43854

Saji, N., and T. Yamagata. 2003. Possible impacts of Indian Ocean Dipole mode events on global climate. *Climate Research* 25:151–169. http://www.int-res.com/abstracts/cr/v25/n2/p151-169/

Webster, P. J., G. J. Holland, J. A. Curry, and H.-R. Chang. 2005. Changes in Tropical Cyclone Number, Duration, and Intensity in a Warming Environment. *Science* 309 (5742):1844–1846. http://www.jstor.org/stable/3843773

Wells, N. 2012. Global Budgets of Heat, Water and Salt. In *The atmosphere and ocean: a physical introduction*, 111–145. Chichester, West Sussex, United Kingdom: Wiley-Blackwell.

Yang, J., Q. Liu, S.-P. Xie, Z. Liu, and L. Wu. 2007. Impact of the Indian Ocean SST basin mode on the Asian summer monsoon. *Geophysical Research Letters* 34 (2). https://agupubs.onlinelibrary.wiley.com/doi/abs/10.1029/2006GL028571

Yuan, J., and J. Cao. 2013. North Indian Ocean tropical cyclone activities influenced by the Indian Ocean Dipole mode. *Science China Earth Sciences* 56 (5):855–865. http://link.springer.com/10.1007/s11430-012-4559-0

Zhang, L., G. Wang, M. Newman, and W. Han. 2021. Interannual to Decadal Variability of Tropical Indian Ocean Sea Surface Temperature: Pacific Influence versus Local Internal Variability. *Journal of Climate* 34 (7):2669–2684. http://libproxy.txstate.edu/login?url=https://search.ebscohost.com/login.aspx?direct=true&db=a9h&AN=149659801&site=eds-live&scope=site

Zheng, X.-T., S.-P. Xie, Y. Du, L. Liu, G. Huang, and Q. Liu. 2013. Indian Ocean Dipole Response to Global Warming in the CMIP5 Multimodel Ensemble. *Journal of Climate* 26 (16):6067–6080. https://journals.ametsoc.org/view/journals/clim/26/16/jcli-d-12-00638.1.xml

50 Years After Hurricane Camille, NOAA Satellites Keep U.S. Weather-Ready. 2019. *NOAA-NESDIS*. https://www.nesdis.noaa.gov/news/50-years-after-hurricane-camille-noaa-satellites-keep-us-weather-ready